Journal of Alloys and Compounds 480 (2009) 802–805

Contents lists available at ScienceDirect

Journal of Alloys and Compounds

journal homepage: www.elsevier.com/locate/jallcom

Carbon combustion synthesis of $LiNi_{0.5}Mn_{1.5}O_4$ and its use as a cathode material for lithium ion batteries

Li Zhang[a], Xiaoyan Lv[b], Yanxuan Wen[a,*], Fan Wang[a], Haifeng Su[a]

[a] School of Chemistry and Chemical Engineering, Guangxi University, Nanning 530004, China
[b] Educational Administration Department, Guangxi University, Nanning 530004, China

ARTICLE INFO

Article history:
Received 24 October 2008
Received in revised form 12 February 2009
Accepted 14 February 2009
Available online 3 March 2009

Keywords:
Lithium ion battery
Cathode material
$LiNi_{0.5}Mn_{1.5}O_4$
Carbon combustion synthesis

ABSTRACT

$LiNi_{0.5}Mn_{1.5}O_4$ has been synthesized by carbon combustion synthesis (CCS) using carbon as fuel. X-ray diffraction (XRD) and scanning electron microscope (SEM) measurements showed that the carbon combustion led to the formation of $LiNi_{0.5}Mn_{1.5}O_4$ with the spinel structure. The structure and particle-size can be adjusted by the amount of carbon used in the CCS. For the $LiNi_{0.5}Mn_{1.5}O_4$ sample prepared with a carbon/Li molar ratio of 0.25, the particle-size distribution fell in the narrow range of 1–2 μm. Electrochemical tests indicated that this $LiNi_{0.5}Mn_{1.5}O_4$ sample delivered a discharge capacity of 131.7 mAh g^{-1} with a capacity retention rate 99.3% after 20 cycles.

1. Introduction

Lithium ion batteries, with transition-metal compounds as cathodes and lithium- or carbon-based anodes, are most attractive as portable power sources for various electronic devices [1–3]. Among numerous transition-metal compounds, manganese oxide-based compounds are particularly attractive as cathodes because of their low cost and non-toxicity. Recently, a series of transition metal-substituted spinel lithium manganese oxides ($LiM_xMn_{2-x}O_4$; M = Cr, Co, Fe, Ni and Cu) have been synthesized [4–8] that have high-voltage plateaus greater than 4.5 V. Among these doped materials, $LiNi_{0.5}Mn_{1.5}O_4$ has received considerable attention because of its good cyclic properties and relatively high capacity, with a plateau at around 4.7 V [7,9,10].

Many approaches have been used to synthesize $LiNi_{0.5}Mn_{1.5}O_4$, including solid-state reactions [10], sol–gel technology [11,12], co-precipitations [13], emulsion drying [14], molten salt technology [15] and spray pyrolysis [16]. However, solid-state reaction synthesis is time-inefficient and energy-ineffective. The product synthesized by this method has irregular morphology, and a broad particle-size distribution [10]. The soft solution process is also unfavorable because it is complicated and employs a number of solvents and organic materials, such as citric acid, ethylene glycol and polyvinyl alcohol.

To get around these limitations, a solution combustion method using a mixture of sucrose and nitrates has been carried out to produce high-quality $LiNi_{0.5}Mn_{1.5}O_4$ [17]. Typically, the exothermic reaction between sucrose and nitrates was used to generate a large amount of heat, which converted the reaction mixture to the oxide precursor, and then the oxide product was obtained by heat-treatment. However, the evaporation of water in this method prolonged the preparation time, which complicated the process.

Self-propagating high-temperature synthesis (SHS) is a particular process leading to the formation of metal alloy and oxide. In this process, a highly exothermic reaction between metal powder and oxidizer generates a high-temperature front that propagates through the reactant mixture, converting them to products [18]. However, SHS cannot be used when the pure metal combustion is either expensive or not highly exothermic, or when the pure metal is either highly pyrophoric or melts at room temperature [19]. Carbon combustion synthesis (CCS) is a modified form of traditional SHS, which uses cheap carbon as fuel rather than the expensive metal [19]. Recently, $LaGaO_3$ [19] and $LiCoO_2$ [20] have been synthesized by CCS.

In this work, we have synthesized the $LiNi_{0.5}Mn_{1.5}O_4$ spinel material by carbon combustion synthesis (CCS). XRD and SEM were used to investigate the effect of the amount of carbon on the particle size and the structure of the $LiNi_{0.5}Mn_{1.5}O_4$ powders. The $LiNi_{0.5}Mn_{1.5}O_4$ powders thus obtained have good electrochemical performance.

2. Experimental

To synthesize $LiNi_{0.5}Mn_{1.5}O_4$ spinel material, Li_2CO_3, NiO and Mn_3O_4 (AR, Beijing Chemical Reagent Co.) at a molar ratio of Li:Ni:Mn = 1.00:0.50:1.50 were thoroughly mixed with carbon in a planetary mill (QM-ISP4). The mixtures were first ignited at 800 °C, and then heated to 900 °C for 3 h before being allowed to cool down to

* Corresponding author. Tel.: +86 771 3233718; fax: +86 771 3233718.
E-mail address: wenyanxuan@vip.163.com (Y. Wen).

0925-8388/$ – see front matter © 2009 Elsevier B.V. All rights reserved.
doi:10.1016/j.jallcom.2009.02.092

RT in air. The phase composition and structure of the powders were identified by X-ray diffraction (XRD, Rigaku D/MAX2500 V diffractometer with Cu Kα radiation), and the particle morphologies of the samples were examined with a scanning electron microscope (SEM, Hitachi S-4500 SEM). FT-IR spectroscopy of the samples was performed using a Nicolet Nexus 470 FT-IR spectrophotometer with a resolution of 4 cm^{-1}. A total of 1.5 mg of the sample dried at 120 °C was thoroughly mixed with 200 mg KBr and pressed into pellets and the scans were performed immediately to avoid water absorption. The frequency range was 700–400 cm^{-1}.

Electrochemical characterizations of the products were performed using CR2032 coin-type cell. The charge–discharge tests of the cells were performed on a CTA2001 battery testing system (Wuhan, China) at 75 mA g^{-1} between 3.3 and 4.9 V (versus Li/Li^+). Slurry was formed by mixing $LiNi_{0.5}Mn_{1.5}O_4$, carbon black and Teflon (PTFE) binder with a weight ratio of 70:20:10. The mixed slurry was coated on to an aluminum current collector. The electrodes were dried under vacuum at 120 °C for 24 h and then punched and weighed. The electrochemical cells were assembled in a glove box under a dry and high purity argon atmosphere. The complete coin cell comprises a cathode, a celgard 2300 as the separator and lithium foil anode. 1 M $LiPF_6$ dissolved in a mixture of ethylene carbonate (EC) and dimethyl carbonate (DMC) (1:1 by volume) was used as the electrolyte.

3. Results and discussion

3.1. XRD analysis

After ignition at 800 °C, the exothermic reaction between carbon and oxygen ($\Delta H = 393.5$ kJ mol^{-1}) in air provides the heat for the solid reactions. The production of $LiNi_{0.5}Mn_{1.5}O_4$ by CCS involves the following reaction:

$$Li_2CO_3 + NiO + Mn_3O_4 + O_2 + \alpha(C + O_2) = 2LiNi_{0.5}Mn_{1.5}O_4 + (\alpha + 1)CO_2\uparrow \quad (1)$$

According to reaction (1), the heat released by the carbon combustion increases with an increase of the amount of carbon, and that causes the increase of the CCS reaction temperature. The combustion features and product properties may be adjusted by amount of carbon in the reactant mixture.

To investigate the effect of the amount of carbon, $LiNi_{0.5}Mn_{1.5}O_4$ powders were synthesized with carbon/Li mole ratios of 0.20, 0.25, 0.35 and 0.50, and the samples obtained were named C-20, C-25, C-35 and C-50, respectively. From Fig. 1, the XRD patterns for the synthesized materials contain the characteristic peaks of the cubic spinel structure. For all products, weak impurity peaks were found at 44° (2θ), and their intensities first decreased and then increased with an increase in the amount of carbon. According to previous reports [7,21], the impurity in the samples should be $Li_xNi_{1-x}O$. The

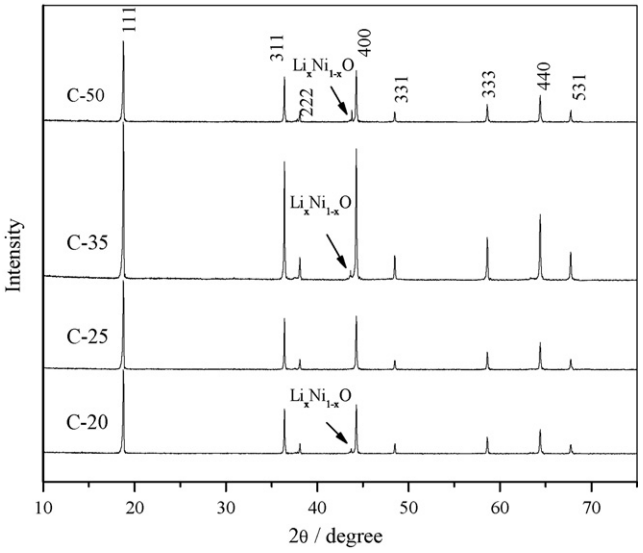

Fig. 1. X-ray diffraction pattern of samples prepared using different carbon/Li mole ratios.

Table 1
Structure parameters of samples prepared using different carbon/Li mole ratios.

Samples	Lattice parameter (Å)	Unit cell volume ($Å^3$)	$I_{(311)}/I_{(400)}$
C-20	8.188	548.95	0.91
C-25	8.175	546.34	0.99
C-35	8.180	547.34	0.96
C-50	8.186	548.55	0.97

impurity in the C-20 sample may be due to insufficient reaction temperature, and that in the other samples may be the result of an excursion to a high temperature environment generated by the carbon combustion. As one part of the Ni^{2+} is removed, the oxidation state of manganese in $LiNi_{0.5}Mn_{1.5}O_4$ decreases, that is, some Mn^{3+} ions appear, which results an increase of the lattice parameter and a discharge plateau at 4 V.

Lattice parameters were calculated with the aim of further investigating the structural factors that are responsible for the electrochemical performance. The impurity phase was not included in the calculation process. The results are summarized in Table 1. It is clear that the lattice parameter at first decreased from 8.188 to 8.175 Å, then increased to 8.186 Å with increase of the carbon/Li mole ratio from 0.2 to 0.5. This result indicates an increase of the amount of Mn^{3+} in the resulting powders when the amount of carbon had exceeded its optimum value.

It has been reported that the intensity ratio of the $I_{(311)}/I_{(400)}$ peaks reflects the structural stability of the $[Mn_2]O_4$ spinel framework [22,23]. The $I_{(311)}/I_{(400)}$ ratio for samples C-25, C-35 and C-50 was higher than 0.95, indicating that these samples show good structural stability. The tiny structural difference may result from the different synthetic conditions formed by the carbon combustion with different carbon/Li mole ratios. Therefore, the structural difference resulting from the intensity ratio of $I_{(311)}/I_{(400)}$ peaks may be closely related to the electrochemical properties of the spinel lithium manganese oxide. Some authors [5,24,25] have reported that Li–Mn–O spinel compounds with $I_{(311)}/I_{(400)}$ ratios between 0.96 and 1.1 have shown better electrochemical properties than those with ratios outside this range. In our work, the $I_{(311)}/I_{(400)}$ ratios for samples C-25, C-35 and C-50 are comparable with those of the Li–Mn–O spinel compounds reported in previous papers [24,25]. Therefore, it is reasonable to expect that these samples will show better electrochemical performance, and this comment is consistent with the results provided below. However, there may be many other factors that affect the electrochemical performance, such as surface morphology and particle size distribution.

3.2. SEM analysis

Fig. 2 shows the SEM images of $LiNi_{0.5}Mn_{1.5}O_4$ prepared using different carbon/Li molar ratios. As the amount of carbon increases, particles with clear octahedral shape were observed. When the carbon/Li mole ratio was 0.20, undeveloped octahedral particles were observed, as shown in Fig. 2(a), which indicate that crystallization toward octahedral shape is in progress. However, when the carbon/Li mole ratio was greater than 0.35, irregular polyhedrons were formed (Fig. 2(c) and (d)). These results suggest that the particle size and morphology of the $LiNi_{0.5}Mn_{1.5}O_4$ can be adjusted by the carbon/Li mole ratio in the CCS. These results show that $LiNi_{0.5}Mn_{1.5}O_4$ prepared by CCS prefers to expose the [1 1 1] face, giving a clear preference for octahedral morphology for the spinel structure [9] due to anisotropy in the surface energy [26].

3.3. FT-IR analysis

Depending on Ni ordering in the lattice, $LiNi_{0.5}Mn_{1.5}O_4$ shows two different space groups, *Fd3m* or $P4_332$ [27,28]. However, this

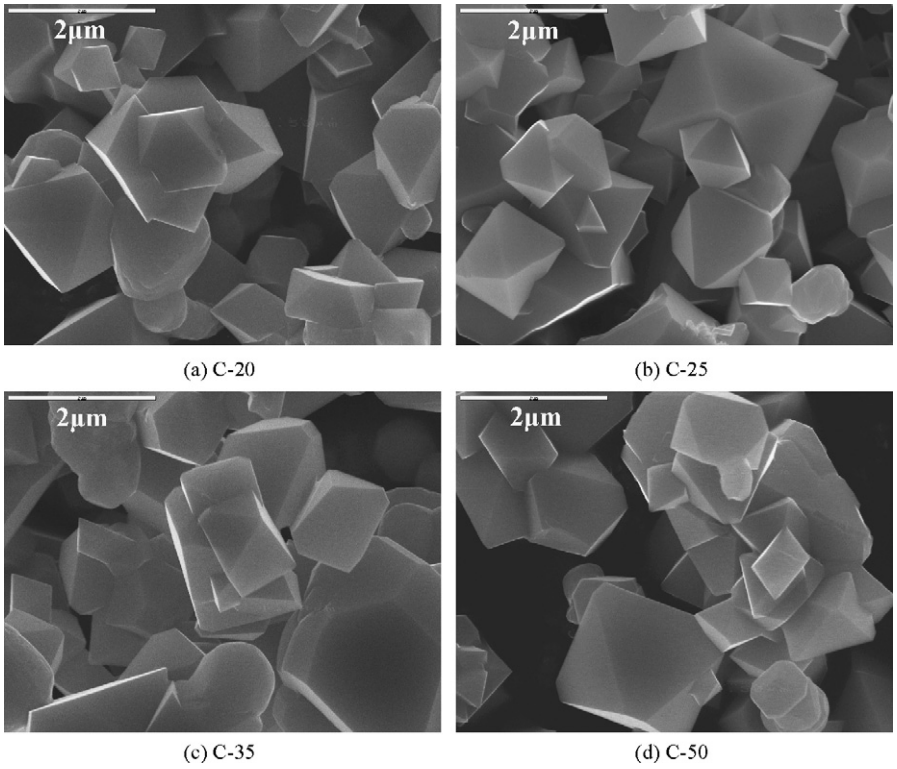

Fig. 2. Micro-morphology of samples prepared using different carbon/Li mole ratios.

structural evolution is hardly seen by XRD because of the similar scattering factors of Ni and Mn. FT-IR spectroscopy has proved to be an effective technique for qualitatively resolving the cation ordering [29,30]. Characteristic infrared vibration bands of the M—O bonds of the sample between 700 and 400 cm^{-1} were used to examine the Ni ordering in $LiNi_{0.5}Mn_{1.5}O_4$. As indicated by the FT-IR spectrum in Fig. 3, sample C-25 showed two bands at 621 and 479 cm^{-1} which are more intense than those at 585 and 470 cm^{-1}. This special feature indicates a disordered structure with the space group *Fd3m* [30]. In addition, the two bands at 649 and 425 cm^{-1} for the $P4_332$ phase were absent or undefined in Fig. 3, which further proves a disordering distribution (*Fd*3*m*) of Ni in the structure of $LiNi_{0.5}Mn_{1.5}O_4$ prepared by CCS.

3.4. Electrochemical performance

Fig. 4 compares the cyclic electrochemical performance of the prepared $LiNi_{0.5}Mn_{1.5}O_4$ over 20 cycles. The discharge capacities of samples C-20, C-35 and C-50 increased with the number of cycles in the initial charge-discharge process. A possible explanation is that there is an activation process caused by the impurity and surface defects in the $LiNi_{0.5}Mn_{1.5}O_4$ obtained by CCS (see Figs. 1 and 2). The cycle-ability first increases and then decreases with increasing the amounts of carbon. When the carbon/Li mole ratio reaches 0.25, the sample obtained achieves the best performance, with a discharge capacity of 131.7 mAh g^{-1} for the first cycle and 130.8 mAh g^{-1} for the 20th cycle.

Fig. 5 shows the charge and discharge curves of the cell with sample C-25. The charge curves exhibit two distinct plateaus at about 4.7 V, which is attributed to the progressive oxidation of Ni^{2+} first to Ni^{3+} and then Ni^{3+} to Ni^{4+} during charge [31]. It is recognized from [25,32] that $LiNi_{0.5}Mn_{1.5}O_4$ with a disordered structure

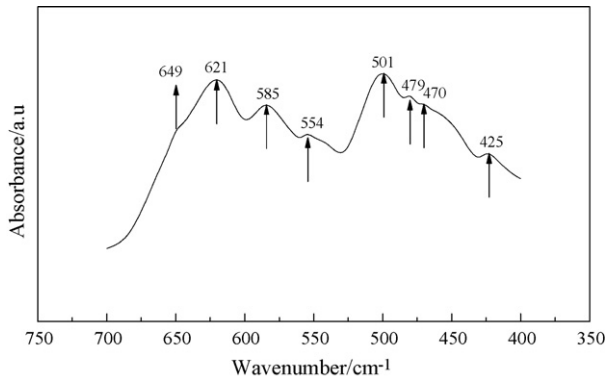

Fig. 3. Fourier transform infrared (FT-IR) spectrum of sample C-25.

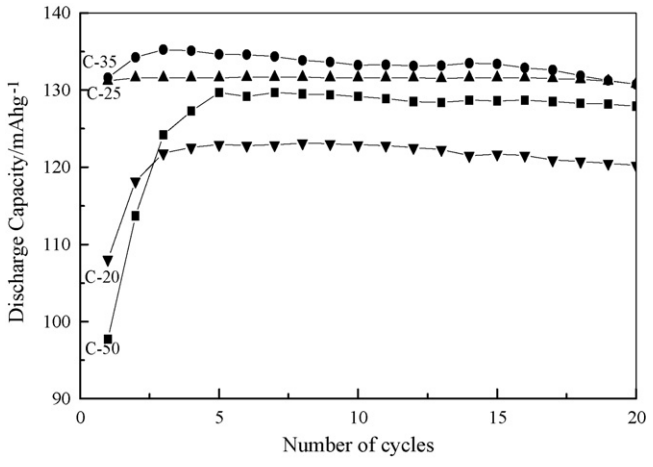

Fig. 4. Capacity vs. cycle number for samples prepared using different carbon/Li mole ratios.

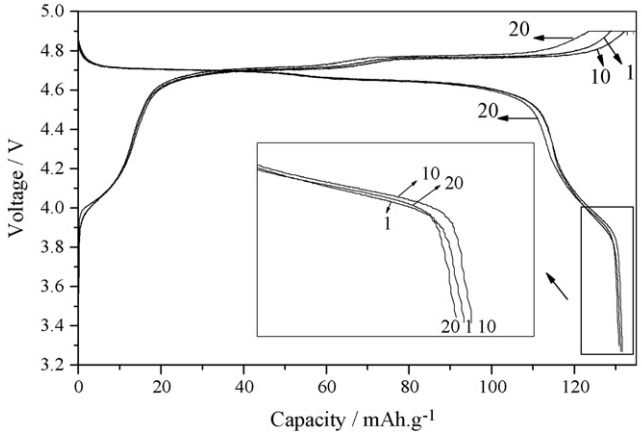

Fig. 5. Charge–discharge profiles of the sample prepared with a carbon/Li mole ratio of 0.25.

(*Fd3m*) would show two obvious voltage plateaus at around 4.7 V while that with an ordered structure ($P4_332$) will give a flat voltage profile at around 4.7 V. Therefore, the observation of two distinct plateaus at about 4.7 V in Fig. 5 confirms the disordered structure of $LiNi_{0.5}Mn_{1.5}O_4$, consistent with the XRD and FT-IR analysis. It is noted that the discharge curves of these samples still present narrower plateaus in the potential region from 3.9 to 4.2 V as well as the two higher voltage plateaus; these result from the transfer reaction between Mn^{3+} and Mn^{4+} [7].

4. Conclusions

We have used a carbon combustion synthesis method to prepare $LiNi_{0.5}Mn_{1.5}O_4$ for lithium ion batteries. All the samples prepared showed a cubic spinel structure with the space group *Fd3m*. The structure and particle-size of the prepared $LiNi_{0.5}Mn_{1.5}O_4$ can be adjusted by the amount of carbon in the CCS. $LiNi_{0.5}Mn_{1.5}O_4$ prepared with a carbon/Li mole ratio of 0.25 showed the largest initial discharge capacity (131.7 mAh g^{-1}) and an excellent capacity retention rate of 99.3% after 20 cycles. The methodology reported in this paper might be extended for the synthesis of a broad class of transition metal oxide materials for lithium ion batteries.

Acknowledgements

The authors appreciate the financial support of the Natural Science Foundation of Guangxi, China (No. 0731010) and the Cooperative Network of the Large-scale Instrument of Guangxi, China (No. 701-2008-114).

References

[1] M. Stanley Whitingham, Chem. Rev. 104 (2004) 4271.
[2] X.Z. Liao, Y.S. He, Z.F. Ma, X.M. Zhang, L. Wang, J. Power Sources 174 (2007) 720.
[3] L.J. Fu, H. Liu, C. Li, Y.P. Wu, E. Rahm, R. Holze, H.Q. Wu, Prog. Mater. Sci. 50 (2005) 881.
[4] W.K. Zhang, C. Wang, H. Huang, Y.P. Gan, H.M. Wu, J.P. Tu, J. Alloys Compd. 465 (2008) 250.
[5] T.F. Yi, Y.R. Zhu, Electrochim. Acta 53 (2008) 3120.
[6] S. Patoux, L. Sannier, H. Lignier, Y. Reynier, C. Bourbon, S. Jouanneau, F.L. Cras, S. Martinet, Electrochim. Acta 53 (2008) 4137.
[7] Q. Zhong, A. Bonakdarpour, M. Zhang, Y. Gao, J.R. Dahn, J. Electrochem. Soc. 144 (1997) 205.
[8] T. Nakamura, H. Demidzu, Y. Yamada, J. Phys. Chem. Solids 69 (2008) 2349.
[9] H.S. Fang, Z.X. Wang, B. Zhang, X.H. Li, G.S. Li, Electrochem. Commun. 9 (2007) 1077.
[10] S.H. Oh, S.H. Jeon, W.I. Cho, C.S. Kim, B.W. Cho, J. Alloys Compd. 452 (2008) 389.
[11] J.C. Arrebola, A. Caballero, L. Hern′an, J. Morales, J. Power Sources 180 (2008) 852.
[12] M. Kunduraci, G.G. Amatucci, Electrochim. Acta 53 (2008) 4193.
[13] Y.K. Fan, J.M. Wang, X.B. Ye, J.Q. Zhang, Mater. Chem. Phys. 103 (2007) 19.
[14] S.T. Myung, S. Komaba, N. Kumagai, H. Yashiro, H.T. Chung, T.H. Cho, Electrochim. Acta 47 (2002) 2543.
[15] J.H. Kim, S.T. Myung, Y.K. Sun, Electrochim. Acta 49 (2004) 219.
[16] S.H. Park, S.W. Oh, S.T. Myung, Solid State Ionics 176 (2005) 481.
[17] R.M. Rojas, J.M. Amarilla, L. Pascual, J.M. Rojo, D. Kovacheva, K. Petrov, J. Power Sources 160 (2006) 529.
[18] A.G. Merzhanov, J. Mater. Chem. 14 (2004) 1779.
[19] K.S. Martirosyan, D. Luss, AIChE J. 51 (2005) 2801.
[20] Y.L. Gan, L. Zhang, Y.X. Wen, F. Wang, H.F. Su, Particuology 6 (2008) 81.
[21] F.G.B. Ooms, E.M. Kelder, J. Schoonman, M. Wagemaker, F.M. Mulder, Solid State Ionics 152–153 (2002) 143.
[22] M.M. Thackeray, Prog. Solid State Chem. 25 (1997) 1.
[23] S.J. Bao, C.M. Li, H.L. Li, J.H.T. Luong, J. Power Sources 164 (2007) 885.
[24] Y.J. Wei, K.W. Nam, K.B. Kim, G. Chen, Solid State Ionics 177 (2006) 29.
[25] Y.S. Lee, N. Kumada, M. Yoshio, J. Power Sources 96 (2001) 376.
[26] M.R. Huang, C.W. Lin, H.Y. Lu, Appl. Surf. Sci. 177 (2001) 103.
[27] J.H. Kim, S.T. Myung, C.S. Yoon, S.G. Kang, Y.K. Sun, Chem. Mater. 16 (2004) 906.
[28] Y. Idemoto, H. Narai, N. Koura, J. Power Sources 119–121 (2003) 125.
[29] R. Alcantara, M. Jaraba, P. Lavela, J.L. Trado, E. Zhecheva, R. Stoyanova, Chem. Mater. 16 (2004) 1573.
[30] M. Kunduraci, J.F. Al Sharab, G.G. Amatucci, Chem. Mater. 18 (2006) 3585.
[31] K.A. Striebel, A. Rougier, C.R. Horne, R.P. Reade, E.J. Cairns, J. Electrochem. Soc. 146 (1999) 4339.
[32] K. Takahashi, M. Saitoh, M. Sano, M. Fujita, K. Kifune, J. Electrochem. Soc. 151 (2004) A173.